Journal of Infrastructure Preservation and Resilience

RESEARCH

Open Access

Evaluating the impact of factors in vehicle based pavement sensing implementation: sensor placement, pavement temperature, speed, and threshold

Dada Zhang[1], Chun-Hsing Ho[1*] and Fangfang Zhang[2]

Abstract

The purpose of the paper is to improve the efficiency of vehicle based sensing technology in highway pavement condition assessment by evaluating the effect of four factors (sensor placement, pavement temperature, drive speed, and threshold for pavement distress classification) and providing suggestions to better improve the accuracy of pavement condition detection and minimize the interruption of pavement sensing operation. Two I-10 corridors in the Phoenix region were selected for vibration data collection and data analysis. A series of statistical analyses were performed to determine if each one of the factors has a significant impact on the pavement distress detection. The results of Analysis of Variance (ANOVA) tests and Analysis of Covariance (ANCOVA) tests show that the placement of sensors have a significant effect in the pavement condition assessments. The significant differences occurred in the group of sensors that were placed on the same side of the vehicle, as well as, in either front wheels or rear wheels of the vehicle. The effect of pavement temperature on the vehicle based sensing implementation is significant while the mean drive speed is not seen as a significant factor in the pavement condition survey. The two thresholds were determined to select points of interest (POI; cracks, potholes) for the pavement distress classification and these POIs are in good agreement with international roughness index (IRI) data in an ArcGIS map. The findings of the paper can be used to better improve the computing algorithms of vehicle based sensing techniques.

Keywords: Pavement condition assessment, ANCOVA, Multiple regression, Vehicle based sensing

Introduction

Evaluating road surface performance required costly equipment and high skilled staff. Traditionally, a roadway profiler has been used by some of governments for pavement condition surveys. The survey result provides longitude roughness data that can be used by highway authorities for decision making for pavement maintenance and repair. Generally, the annual costs of obtaining roughness data and condition surveys could be more than one hundred thousand dollars [1] which is not affordable for most of highway agencies who have a need but with limited budget to conduct pavement condition surveys. To approach a low-cost and efficient monitoring system, the use of vibration data instead of pavement roughness index via different methodologies has been given attention in road condition assessment among highway agencies and institutes. There are two commonly used methods to collect vibration data; the first one being a smartphone based sensors, which is a convenient and easy way to gain acceleration data while another one is a vehicle mounted sensor used to collect pavement sensing patterns and signals according to their demands. Many research studies showed that there

*Correspondence: chunhsing.ho@unl.edu

[1] Durham School of Architectural Engineering and Construction, College of Engineering, University of Nebraska – Lincoln, Lincoln, NE 68588, USA
Full list of author information is available at the end of the article

is a correlation between acceleration data and pavement roughness [2–6]. Thus, using accelerometers equipped in a smartphone or vehicle has been widely used in pavement condition surveys.

Ho et al. [7] and Zhang et al. [8] conducted a year-long pavement condition survey using vehicle based pavement sensing techniques on the I-10 corridors in the Phoenix region. Their findings are strongly in support of vehicle mounted sensors for use in pavement condition assessment. Based on their study, there are still some factors that could have an impact on the accuracy of pavement condition detection such as tire pressure, drive speed, placement of sensors, threshold for pavement distress classification, etc. Thus, a further investigation on how these factors would influence the implementation of vehicle based sensing work is needed.

Literature review

Road roughness and pavement condition index are two common parameters in pavement condition evaluation. Usually, the vehicle-mounted sensors are applied in a pavement condition survey to obtain roughness index through a specified automated methodology [9], however, which requires costly equipment and high skilled staff. A report also studied the relation between the roughness index and the pavement condition index (PCI) via visual inspection of different types of road deterioration [10]. However, field observation and rating heavily reply on human power and the results might not be consistent among field raters. Due to the limited budget and labor, highway agencies have been in search of a cost effective way to find an affordable pavement condition survey method such as accelerometers, real-time images, etc. A study by Yan et al. indicated that the acceleration signals have a significant effect on the deeper and longer cracks in the pavement condition [11]. A report by Alavi et al. expressed that the vertical acceleration data from a smartphone can be used in assessing overall airport pavement condition [12]. Moreover, Douangphachanh et al. indicated that the acceleration vibration data has a good linear relationship with PCI values [3, 6] and is correlated with roughness index [2]. These are evident that the use of accelerometers in pavement condition assessment has been dramatically increased.

To precisely analyze vibration signals and transfer the results in to the pavement distress classifications, a variety of computing algorithms have been used in the determination of pavement distress such as numerical analysis, supervised machine learning, and image processing through MATLAB software [11–18]. For example, Fast Fourier transform (FFT) and Short-term Fourier Transform (STFT) have been used to find the displacement data based on the vertical acceleration for evaluating road performance [5, 17]. Their results indicated that higher displacement values, and poor road conditions, visually matched with road conditions. Through numerical analysis of vertical acceleration, Yan et al. found that most cracks have positive vertical acceleration in pavement condition assessments [11] and the cracks can be identified by integrating the differential intensity and height changes from the data [19]. Additionally, using polynomial approximation is another way to determine the locations of potholes in the condition assessment [20]. More recently, machine learning based techniques have become a widely used method in road condition assessment. For example, k-nearest neighbor (KNN) is one of common and simple machine learning approaches to classify pavement conditions. Du et al. used the KNN method to distinguish the abnormal pavement types such as bump and pothole, and the results showed that the accuracy of the recognition is more than 90%, which proved the vibration data was appropriate to be processed in the condition assessment [13]. Additionally, Artificial Neural Network (ANN), fuzzy theory, and random forests regression have been broadly applied by numerous scholars to recognize road surface conditions for maintenance and rehabilitation purposes [14, 16, 21, 22].

Recent studies have suggested that using vertical accelerations from a single device or sensor to assess pavement conditions is not sufficient to facilitate pavement distress classification [7, 8, 23, 24]. Thus, the use of multiple devices or sensors in vibration data collections have been used in several studies. For instance, Staniek indicated the use of three-dimensional analysis of acceleration vibrations could lead to a better and precise calculation for pavement condition indices [24]. To recognize the abnormal pavement performance, Chuang et al. used a deep machine learning technique associated with vertical and lateral acceleration [23] and their results were successfully validated by the road network of Taipei city, Taiwan with an accuracy of 98%. Additionally, the bagged trees classification and robust regression analysis were applied in pavement monitoring through three-dimensional rotations and the results of detection exhibited accuracy of more than 90% [25]. Ho et al. [7] and Zhang et al. [8] used magnitude values, which was combining all three accelerations in the three directions to monitor pavement conditions and their results were effectively validated with IRI segments.

Given all above studies, it is clearly the use of accelerometers is getting popular among highway agencies and institutes for its affordable costs and reasonable results in pavement condition classifications. However, the factors that could have influenced the accuracy of pavement distress detection have not well studied yet. To address

these issues and better support the implementation of vehicle based sensing work, the paper evaluates the effect of the factors (sensor placement in vehicle, pavement temperature, drive speed, and thresholds for pavement distress classification) on the implementation of vehicle based sensing techniques using statistical analyses. The objectives of the paper are to:

1. evaluate the effect of individual factor on the pavement sensing operation and provide suggestions to minimize its effect on the interruption of pavement condition and
2. support the currently used vehicle based sensing techniques in the pavement condition survey.

This paper presents statistical analysis using both analyses of variance and analysis of covariance to evaluate the effect of different factors such as sensor placement, pavement temperature, speed, and threshold in pavement condition assessments based on a year-long data set.

Methods

Data acquisition

Two road sections were selected in Phoenix, Arizona for pavement condition surveys that are shown in Fig. 1. The length of road Sect. 1 (51st Ave to 27th Ave) is 3 miles and two lanes on eastbound (EB) were selected. Similarly, two lanes on northbound (NB) were selected in road Sect. 2 (Chandler Blvd to Baseline Rd), and each of the lane has a length of 5 miles. All pavement sensing patterns and signals were collected monthly in a year long through multiple sensors by a 2016 Honda Accord. As shown in Fig. 2, sensors M1 to M4 were placed on the top of each control arm of the vehicle, and M5 was placed inside of the vehicle to gather sensing patterns simultaneously during travelling on the two road sections. A GoPro was attached to the front of the vehicle to record the real-time pavement conditions such as cracks, detection loop, and construction joints. The video is applied in the validation of pavement deterioration along with the IRI file for further pavement condition classification.

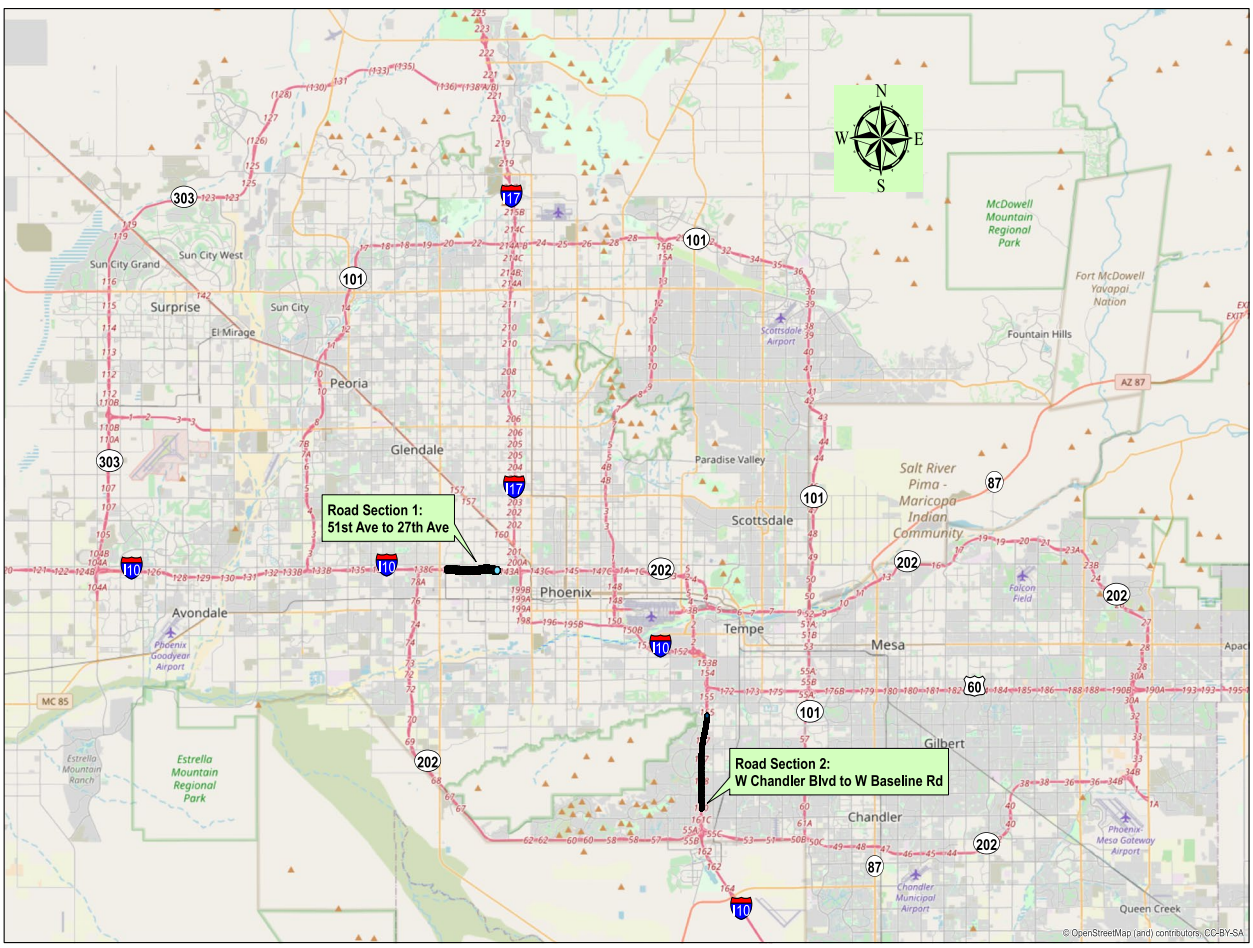

Fig. 1 Road sections in pavement condition surveys on the I-10 corridor in Phoenix, AZ. Source: https://cdn.arcgis.com/sharing/rest/content/items/0df19d2d940b47658857cc2fc9623840/resources/styles/root.json

Fig. 2 Sensor placements prior to field data collection. Note: M1 and M2 were placed on the front wheels of the vehicle, M3 and M4 were placed on the rear wheels of the vehicle. The vehicle in the figure is an example to show the sensor placement

Table 1 A Sample of pavement sensing file

ACCTIME	2017–03-25 02:34:40:003	2017–03-25 02:34:40:034	2017–03-25 02:34:40:066
XG1	-0.0880	0.0196	0.0196
YG1	0.2151	0.1369	0.1271
ZG1	-0.1662	0.0782	-0.1662
M1	0.2857	0.1588	0.2101
XG2	-0.1955	-0.1173	-0.2053
YG2	-0.0880	0.0391	0.0782
ZG2	-0.3715	-0.4790	-0.1369
M2	0.4289	0.4947	0.2588
XG3	0.1173	0.1173	0.0196
YG3	-0.2444	0.3128	0.1662
ZG3	0.0489	-0.1075	-0.0391
M3	0.2754	0.3510	0.1718
XG4	-0.3715	-0.2542	-0.3226
YG4	-0.0196	0.0587	0.2835
ZG4	-0.1760	-0.1760	-0.1075
M4	0.4115	0.3146	0.4427
XG5	0.0293	0.0391	0.0196
YG5	0.1857	0.1369	0.2639
ZG5	-0.0293	-0.0587	0.0489
M5	0.1903	0.1539	0.2691
LAT	33.4623942	33.4623942	33.4623942
LNG	-112.1637207	-112.1637207	-112.1637207
ALT	323.399994	323.399994	323.399994
SPEED	59.38	59.38	59.38

LAT, LNG, and ALT represent latitude, longitude, and altitude in geographic coordinates

Table 1 is a sample of pavement sensing files, which includes acceleration vibrations from three directions (e.g. x, y, and z), GPS coordinates, time, driving speed, and magnitude values from all five sensors. The details about the data collection process are explained in references [7, 8]. In the pavement condition assessment, the driving speed was maintained from 50 to 55 miles per hour except for the traffic congestion that occurred. Also, the pavement temperature was recorded by an infrared thermometer during each pavement condition survey.

Data application

To meet assumptions of normality in statistical tests, all magnitude values were transformed into a logarithm scale. Figure 3 illustrates the density plots of the transformed data (e.g. logM). It is clear to see that the distributions of sensor 5 are significantly different than other sensors due to the placement in the pavement condition assessments.

Data analysis

This section introduces the methodologies that were used to evaluate the effect of sensors in the pavement sensing work and to determine the significant variables such as pavement temperature and mean speed that have an impact on the pavement condition assessment.

Effect of sensor placements in pavement condition assessment

To further investigate the effect of sensors in the pavement sensing work, the paper perform ANOVA tests associated with the cell means model through the following [26]:

$$y_{ij} = \mathrm{EE}\mu_i + e_{ij}, i = 1, 2, \ldots, tandj = 1, 2, \ldots, r \quad (1)$$

where.

y_{ij} = magnitudes in log scale of j^{th} months from the i^{th} sensors;

μ_i = mean for all magnitudes from the i^{th} sensor;

e_{ij} = random error.

In the study, the random error was assumed to be independent identically distributed to a normal distribution with zero mean and constant variance in order to provide valid statistical inference.

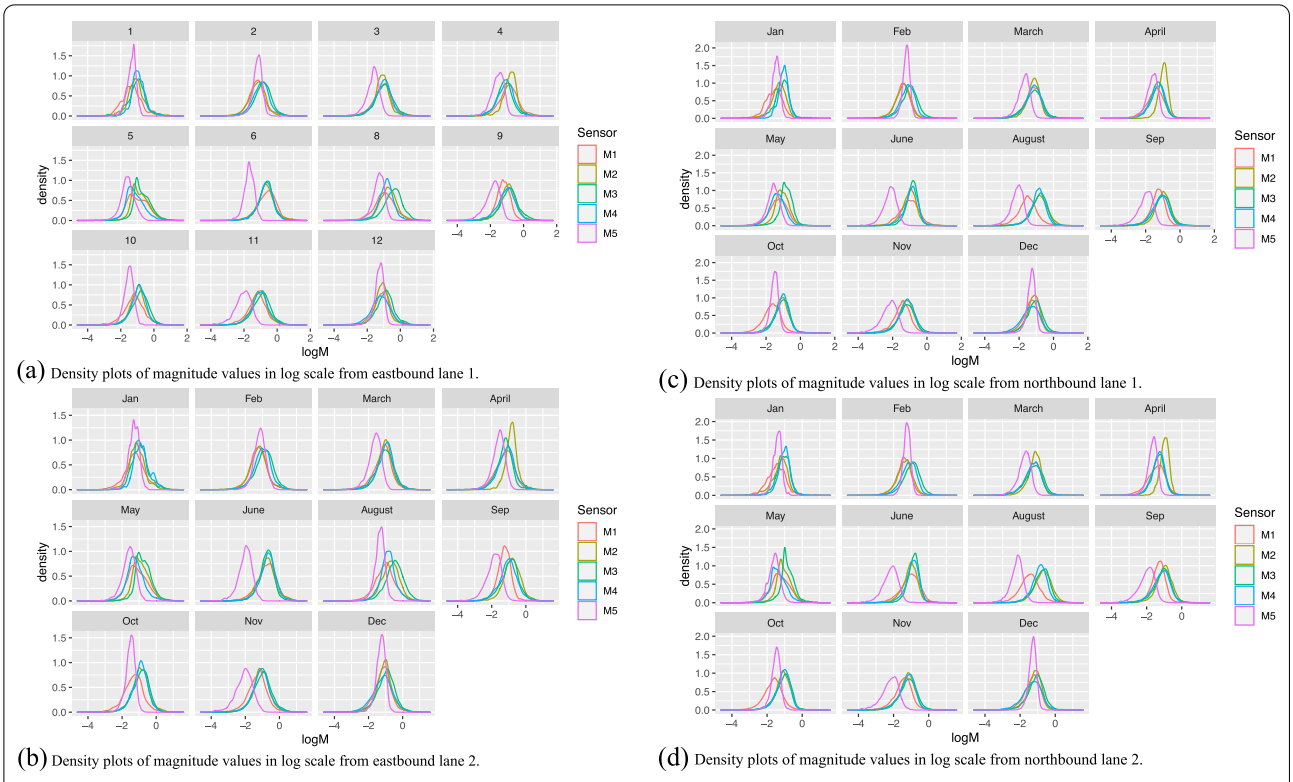

(a) Density plots of magnitude values in log scale from eastbound lane 1.

(c) Density plots of magnitude values in log scale from northbound lane 1.

(b) Density plots of magnitude values in log scale from eastbound lane 2.

(d) Density plots of magnitude values in log scale from northbound lane 2.

Fig. 3 Density plots of magnitude values in log scale from two road sections. **a** Density plots of magnitude values in log scale from eastbound lane 1. **b** Density plots of magnitude values in log scale from eastbound lane 2. **c** Density plots of magnitude values in log scale from northbound lane 1. **d** Density plots of magnitude values in log scale from northbound lane 2

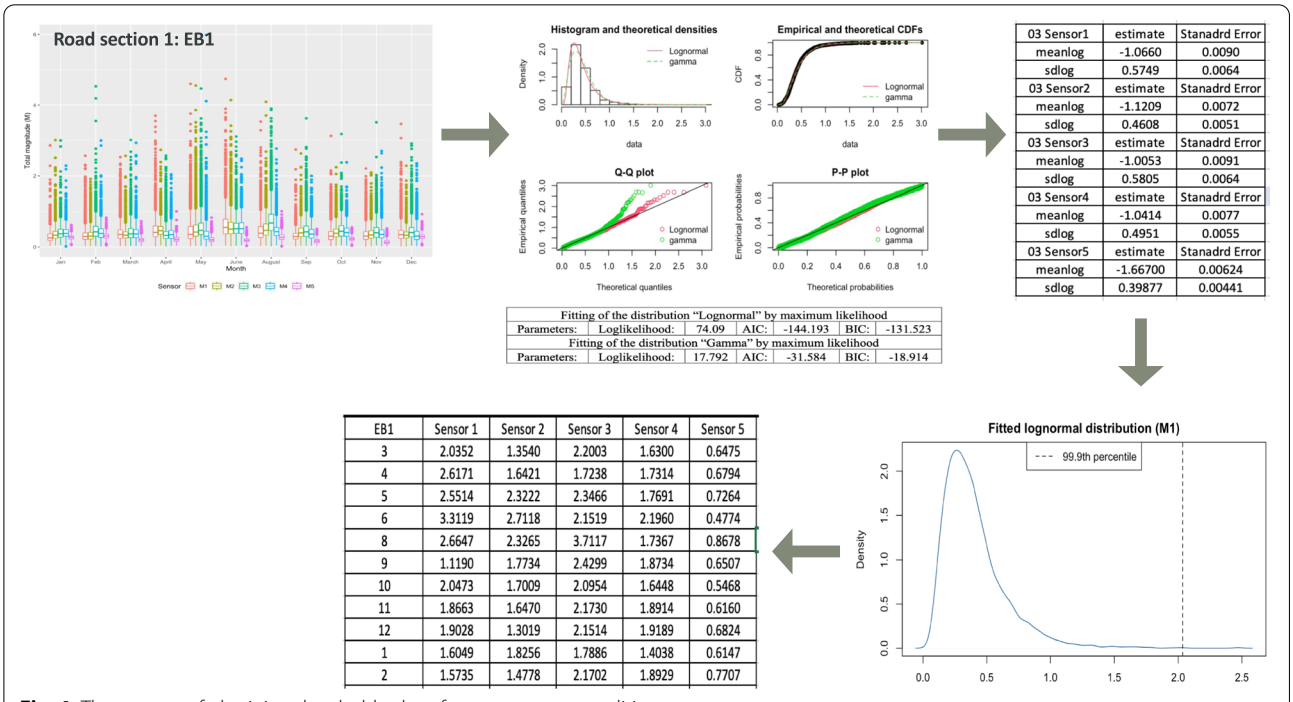

03 Sensor1	estimate	Stanadrd Error
meanlog	-1.0660	0.0090
sdlog	0.5749	0.0064
03 Sensor2	estimate	Stanadrd Error
meanlog	-1.1209	0.0072
sdlog	0.4608	0.0051
03 Sensor3	estimate	Stanadrd Error
meanlog	-1.0053	0.0091
sdlog	0.5805	0.0064
03 Sensor4	estimate	Stanadrd Error
meanlog	-1.0414	0.0077
sdlog	0.4951	0.0055
03 Sensor5	estimate	Stanadrd Error
meanlog	-1.66700	0.00624
sdlog	0.39877	0.00441

EB1	Sensor 1	Sensor 2	Sensor 3	Sensor 4	Sensor 5
3	2.0352	1.3540	2.2003	1.6300	0.6475
4	2.6171	1.6421	1.7238	1.7314	0.6794
5	2.5514	2.3222	2.3466	1.7691	0.7264
6	3.3119	2.7118	2.1519	2.1960	0.4774
8	2.6647	2.3265	3.7117	1.7367	0.8678
9	1.1190	1.7734	2.4299	1.8734	0.6507
10	2.0473	1.7009	2.0954	1.6448	0.5468
11	1.8663	1.6470	2.1730	1.8914	0.6160
12	1.9028	1.3019	2.1514	1.9189	0.6824
1	1.6049	1.8256	1.7886	1.4038	0.6147
2	1.5735	1.4778	2.1702	1.8929	0.7707

Fig. 4 The process of obtaining threshold values from pavement condition assessments

Table 2 Results of ANOVA tests on four sensors for two road sections

Analysis of Variance Table EB1					
	Df	Sum Square	Mean Square	F value	*P*-value
Sensor	4	41.945	10.486	334.94	< 2.20E-16
Residuals	40	1.252	0.0313		
Analysis of Variance Table EB2					
	Df	Sum Square	Mean Square	F value	*P*-value
Sensor	4	45.076	11.269	389.48	< 2.20E-16
Residuals	40	1.157	0.0289		
Analysis of Variance Table NB1					
	Df	Sum Square	Mean Square	F value	*P*-value
Sensor	4	61.646	15.4115	585.65	< 2.20E-16
Residuals	40	1.053	0.0263		
Analysis of Variance Table NB2					
	Df	Sum Square	Mean Square	F value	*P*-value
Sensor	4	62.129	15.532	539.54	< 2.20E-16
Residuals	40	1.152	0.0288		

EB represents eastbound and NB represents northbound

The Tukey's test was applied for pairwise comparison to determine where the significant differences occur associated with small p-values such as less than 0.05 (or less than 0.10). In the paper, the TukeyHSD function [27] in R software was applied to conduct 95% confidence intervals and to investigate the significant difference in various groups based on simultaneous pairwise comparisons.

Effect of pavement temperature and drive speed in pavement condition assessment

The factorial treatment design was used to investigate the relationships among several types of treatments and various conditions [26]. In the paper, the Analysis of covariance (ANCOVA) tests were performed based on the factorial design to examine the interaction between sensors, pavement temperature, or mean speed in pavement condition surveys. Three statistical models were built synchronously including the simple regression model, main effects model, and interaction model to access the interaction effects. The simple regression model [28] can be written as below:

$$y = \beta_0 + \beta_1 X_1 + \varepsilon \tag{2}$$

where.
y = mean magnitude in log scale;
β_0 = intercept;
β_1 = regression coefficient as known as the slope;
X = inputs;
ε = estimated error.

The main effects model and interaction model were constructed to address the ANOVA tests and ANCOVA tests in the paper. The main effects model can be written as follow [28]:

$$y = \beta_0 + \beta_1 X_1 + \beta_2 X_2 \tag{3}$$

where.
y = mean magnitude in log scale;
β_i = estimated coefficients from the model;
X_i = inputs that consist of sensor and pavement temperature.

To test the interaction of the sensor and pavement temperature or sensor and speed, a model can be written as below:

$$y_{ijk} = \mu + \alpha_i + \beta_j + (\alpha\beta)_{ij} + e_{ijk} \tag{4}$$

where.
y_{ijk} = mean magnitude in log scale of k^{th} months with the j^{th} pavement temperature.
(or mean speed) from the i^{th} sensors;
μ = overall mean;
α_i = fixed effect of the i^{th} sensor;
β_j = fixed effect of the j^{th} pavement temperature (or mean speed);
$(\alpha\beta)_{ij}$ = interaction effect of the i^{th} sensor and the j^{th} temperature (or mean speed);
e_{ijk} = experimental error.
In the paper, an experimental error is assumed to be independent identically distributed to a normal distribution with zero mean and a constant variance [26].

Additionally, a hypothesis test is necessary to be constructed along with the ANCOVA tests to test the interaction of two variables through following form:

$$H_0^{(I)} : (\alpha\beta)_{ij} = 0 vs. H_a^{(I)} : atleastone(\alpha\beta)_{ij} \neq 0 \tag{5}$$

$$Teststatistics : F^{(I)} = \frac{MS(AB)}{MSE} \tag{6}$$

where.
$(\alpha\beta)_{ij}$ = interaction effect of the i^{th} sensor and the j^{th} temperature (or mean speed);
MS(AB) = mean square of sensors and pavement temperature (or mean speed);
MSE = mean square of error.
Reject the null hypothesis (e.g. no sensor × pavement temperature interaction effects) if the p-value is small (e.g. less than 0.10) and conclude that the interaction effects exist. When the interaction effect exists, the result of the main effects is not to be discussed in detail. If the intersection effects are not significant, discuss the results

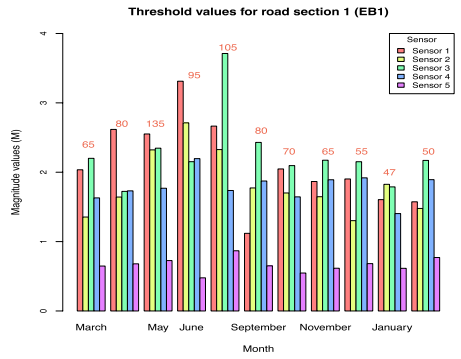

(a) Threshold values from eastbound lane 1.

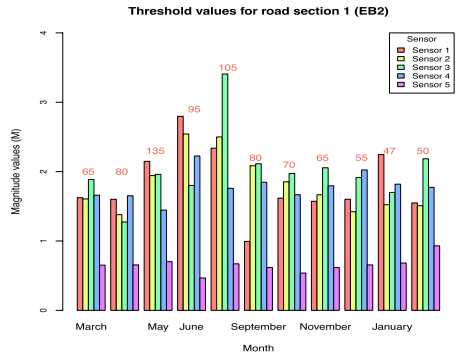

(b) Threshold values from eastbound lane 2.

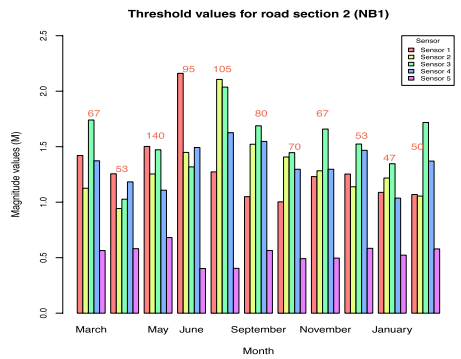

(c) Threshold values from northbound lane 1.

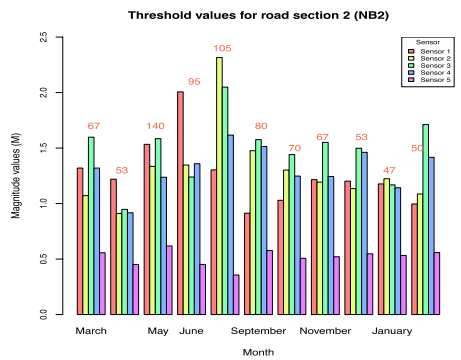

(d) Threshold values from northbound lane 2.

Fig. 5 Threshold values for two road sections. **a** Threshold values from eastbound lane 1. **b** Threshold values from eastbound lane 2. **c** Threshold values from northbound lane 1. **d** Threshold values from northbound lane 2. Note: the values on the top of the bar plot indicate the pavement temperature (Fahrenheit)

of the main effect model and conclude that the predictors (sensor, pavement temperature, or speed) have effect on the magnitudes if the *p*-value is small (e.g. less than 0.10).

The effect of thresholds in pavement condition assessment

Referring to the authors' previous work [7, 8], the threshold values that classify the pavement condition were obtained from distribution fitting and percentile analysis. Figure 4 illustrates the process of obtaining threshold values from eastbound lane 1 in road Sect. 1 (51st Ave. to 27th Ave). A fitdistrplus package in R software was used to find the best distribution models based on the magnitude values from five sensors (e.g. M1 to M5). Then computing the 99.9th percentile from the fitted models and the corresponding values are defined as thresholds. The remaining 0.1 percent of the data would indicate pavement deterioration. Additionally, the paper analyzed a single sensor (e.g. M5) individually for condition assessments. The concept of this new method is constructing 95% confidence intervals to determine untypical points using standardization data, and those untypical points would indicate pavement deterioration in the condition assessments.

Results and discussion

This section depicts all results and discussion from the proposed methodologies to assess pavement conditions. The results of sensor effects in condition assessments and determination of threshold values are shown in Tables 2 to 8 associated with Figs. 5 to 6.

Results in sensor placement effect

With the elimination of sensor 5, ANOVA tests and Tukey's tests were conducted as expressed in Eq. (1), and the results are shown in Tables 2 and 3. The means of magnitudes in the log scale from four sensors (M1 to M4) differ according to small *p*-values (Table 2). The pairwise comparisons from Tukey's tests show that the means of sensor 1 that is mounted on the front left side of the vehicle differs from the means of the rest sensors for both lanes in road Sect. 2 and eastbound lane 1 in road Sect. 1 due to the *p*-values are less than 0.05 as shown in Table 3.

Moreover, ANOVA tests were performed again to determine whether or not there is a significant difference between the sensors that are mounted on the same

side of the vehicle such as front (or rear) wheels and left (or right) side. As shown in Table 4, the small *p*-values (e.g. less than 0.05) indicate that the mean magnitudes of two sensors that mounted on the same side of the vehicle (e.g. M1 and M3) differ in log scale, as well as, the sensors on either front wheels or rear wheels of the vehicle. Therefore, the paper concludes that the placements of sensors have a significant effect on the measurements of road performance and the effect of sensor 1 that is mounted on the left front wheel of the vehicle is most significant in pavement condition surveys than the rest of the sensors (e.g. M2, M3, and M4).

Results in interaction effects of sensor, pavement temperature, and mean speed

The simple regression model, main effect model, and interaction model were compared simultaneously in the paper as indicated in Table 5. For both road sections, the interaction models of sensors and pavement temperature are significant at the significance level of 0.10 since the *p*-values are less than 0.10. Thus, the paper concludes that the effect of sensors depends on the pavement temperature in the pavement condition surveys. However, the *p*-values are not small (e.g. greater than 0.10) from the interaction models and main effect models when testing the interaction of sensors and mean speed. Therefore, the result indicates that the mean speed is not an important factor in the pavement condition assessment.

Additionally, the *p*-values from the intersection of sensor 4 and pavement temperature for road Sect. 1 are 0.419 and 0.384 (Table 6), for road Sect. 2 are 0.076 and 0.060 (Table 6), which indicate that the interaction effect of sensor 4 and pavement temperature exist less significantly than other groups and provide lower magnitude values in pavement condition surveys.

The paper aims to classify pavement conditions based on a preselected threshold value. However, since the means of vibration responses from the five sensors vary depending on the pavement temperature, it is somewhat difficult to appropriately determine a threshold value based on a year-long data set. Thus, the paper used data collected in the winter season from October to the following February intending to determine a threshold for pavement condition assessment. In this case, the ANOVA and ANCOVA tests were performed again to test the interaction of sensor and pavement temperature in the winter season. As shown in Table 7, all *p*-values are greater than 0.10, which indicate the effect of sensing data on the pavement temperature is not significant in the winter season (October to the following February) in pavement condition assessments.

Results in threshold values in pavement distress classification

Figure 5 shows all threshold values that were used to classify pavement conditions in two road sections. The pavement surface temperature was also shown in the figures and it was noticed that the determination of threshold values varies based on statistical analysis. As shown in Fig. 5, the maximum threshold values occurred in June and August in both road sections that were caused by higher pavement surface temperature. At the same time, the trend of threshold values from all sensors is approximately flat in both sections in the winter (October to February). Therefore, the paper suggests a winter season might be a good time to collect vibration data to avoid pavement temperature effects in assessing pavement conditions while using a constant threshold value to implement pavement distress classification.

Table 8 shows all thresholds from sensors 1 to 4 that were placed on the control arms of the vehicle. Referring to the above analysis, the paper only analyzed the thresholds in the winter season (e.g. October to the following February) to calculate an average threshold value for determining the poor pavement condition in two road sections using the following equations:

$$EB_{threshold} = \frac{ET_{10} + ET_{11} + ET_{12} + ET_1 + ET_2}{n} \tag{7}$$

$$NB_{threshold} = \frac{NT_{10} + NT_{11} + NT_{12} + NT_1 + NT_2}{n} \tag{8}$$

where.

$EB_{threshold}$ = mean threshold in road Sect. 1;

$NB_{threshold}$ = mean threshold in road Sect. 2;

ET_i, NT_i = threshold values computed from the fitted distribution models;

i = 10, 11, 12, 1, and 2 that represent the month in data collection period.

As shown in Table 8, the means of the thresholds from sensors 1 to 4 on eastbound lanes are 1.83, 1.84, 1.78, 1.74, and 1.77. Then the average threshold can be computed by Eq. (7) and $EB_{threshold} = \frac{1.83+1.84+1.78+1.74+1.77}{5} = 1.79$. Similarly, the average threshold for northbound lanes is $NB_{threshold} = \frac{1.27+1.33+1.34+1.18+1.31}{5} = 1.28$ (Eq. (8)).

(See figure on next page.)

Fig. 6 Poor pavement condition through multiple sensors in two road sections. **a** Poor pavement condition through multiple sensors (road Sect. 1). **b** Poor pavement condition through multiple sensors (road Sect. 2). Note: the selected significant points in the circle are validated through recorded video. **c** The significant points correspond to the road condition in road Sect. 2. Source: https://cdn.arcgis.com/sharing/rest/content/items/0df19d2d940b47658857cc2fc9623840/resources/styles/root.json

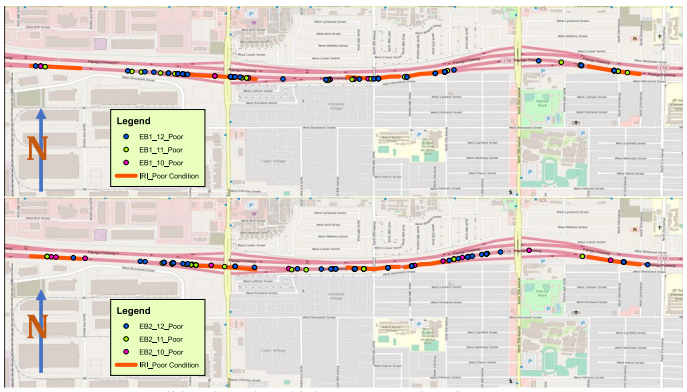

(a) Poor pavement condition through multiple sensors (road section 1).

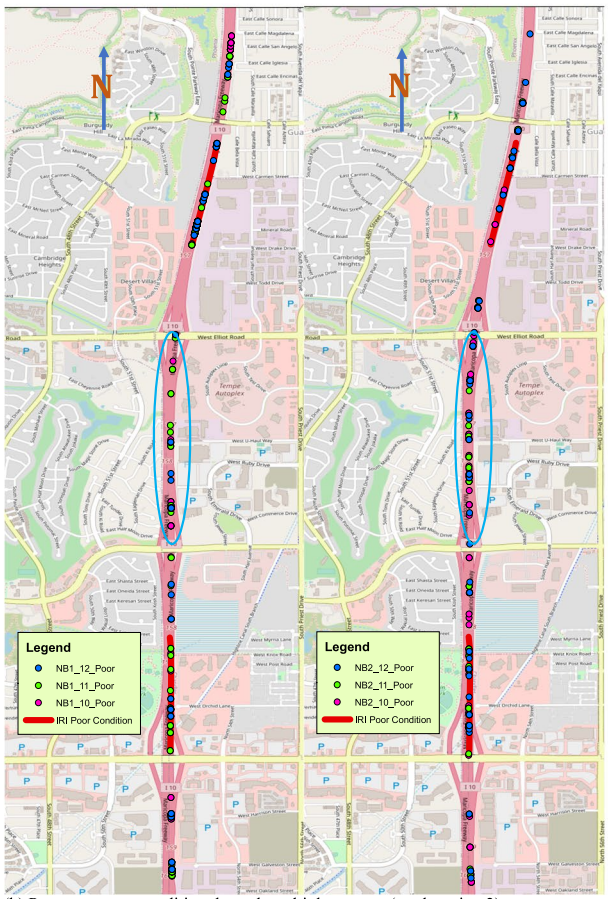

(b) Poor pavement condition through multiple sensors (road section 2).
Note: the selected significant points in the circle are validated through recorded video.

Northbound lane 1

Northbound lane 2

Fig. 6 (See legend on previous page.)

Table 3 Results of Tukey's test on four sensors for multiple comparisons

Pairwise comparisons (95% C.I.) NB1					Pairwise comparisons (95% C.I.) NB2				
group	difference	lower	upper	*p*-value	group	difference	lower	upper	*p*-value
2–1	0.109	0.093	0.311	**0.049**	2–1	0.212	0.017	0.406	**0.028**
3–1	0.216	0.013	0.418	**0.033**	3–1	0.251	0.056	0.445	**0.007**
4–1	0.071	-0.131	0.273	0.785	4–1	0.159	-0.035	0.354	0.142
3–2	0.107	-0.096	0.309	0.499	3–2	0.039	-0.156	0.233	0.950
4–2	-0.038	-0.241	0.164	0.957	4–2	-0.053	-0.247	0.142	0.886
4–3	-0.145	-0.347	0.057	0.236	4–3	-0.091	-0.286	0.103	0.592
2–1	0.262	0.077	0.448	**0.003**	2–1	0.272	0.078	0.466	**0.003**
3–1	0.320	0.134	0.505	**0.000**	3–1	0.318	0.124	0.511	**0.000**
4–1	0.231	0.045	0.416	**0.010**	4–1	0.211	0.017	0.405	**0.028**
3–2	0.057	-0.128	0.243	0.841	3–2	0.046	-0.148	0.240	0.921
4–2	-0.032	-0.217	0.154	0.968	4–2	-0.060	-0.254	0.133	0.837
4–3	-0.089	-0.274	0.097	0.579	4–3	-0.106	-0.300	0.088	0.466

Comparison of proposed threshold values with IRI data

The paper used the mean threshold values of 1.79 g and 1.28 g to identify pavement distress points (known as points of interest, POI) in the raw data for the winter season (October to the following February) in the two road sections. Those selected POI were imported in ArcGIS software and graphically illustrated in Fig. 6. An IRI data was obtained from ADOT for comparison with the selected POI, and the correlation between select POI and IRI values are shown in Fig. 7. In this case, IRI values exceeding 95 is identified as a fair to poor condition were selected and graphed in a GIS map [29]. As can be seen in the road Sect. 1 of Fig. 6, poor IRI segments are in good match with the selected POI using the proposed threshold value. As for road Sect. 2, it is noticed that there is a segment circled in blue where the selected POI were displayed without IRI being appeared. This difference in an identification of pavement distress needs a further verification so allowing the team to make a decision. A video made by Go-Pro was retrieved and the team was able to locate the area and made a few snap shots of images that show pavement surface conditions (Fig. 6c). Obviously, the images show deteriorated road surface conditions in support of the selected POI on a map. It can be concluded that the proposed threshold values are valid and effective in the pavement distress classification based on the comparison with IRI and the verification of field images.

Conclusions

The paper intends to evaluate the four factors (placement of sensors, temperature, mean speed, and threshold values) influencing the accuracy of pavement condition detection has the following conclusions through proposed methodologies:

1. The mean of magnitude values in log scale from sensors 1 to 4 differ in the pavement condition surveys through ANOVA tests (Table 2). Among four sensors amounted in the vehicle, Sensor 1 has the most significant difference from other sensors based on the Tukey's tests (Table 3) in the pavement condition assessments.
2. The differences between sensors on the same side of the vehicle (e.g. left or right side, front or rear wheels) are significant in pavement condition surveys due to small p-vales from ANOVA tests (Table 4).
3. Through ANCOVA tests, the interaction effect of sensors, pavement temperature, and mean speed in condition assessments were investigated. The effect of pavement temperature on the pavement distress detection is significant based on small *p*-values occurred in interaction models (Table 5) in two road sections. the paper also suggested to collect vibration data during the winter season to reduce the effect of pavement temperatures in the pavement distress detection.
4. The effect of the mean speed in the pavement distress detection is not an important factor given the fact that larger *p*-values were calculated from main effect model and interaction model (Table 5).
5. Two thresholds (1.79 g for the section of 27th Ave. to 51st Ave and 1.28 g for the section of Baseline Rd. to Chandler Blvd.) were determined using statistical analysis to select POIs. Based on GIS mapping, these POIs are in good agreement with IRI data. The results indicate the threshold values are valid and effective in the detection of deteriorated pavement conditions.
6. The findings of the paper can be used to better improve the computing algorithm of vehicle based pavement sensing techniques.

Table 4 Results of ANOVA tests on two sensors that mounted on the same side of the vehicle for two road sections

	Df	Sum Sq	Mean Sq	F value	*P*-value
Road Sect. 1: EB1 sensor 1 and sensor 3					
Sensor	2	20.7128	10.3564	274.95	2.83E-15
Residuals	20	0.7533	0.0377		
Road Sect. 1: EB1 sensor 2 and sensor 4					
Sensor	2	21.232	10.6159	425.49	2.20E-16
Residuals	20	0.499	0.0249		
Road Sect. 1: EB2 sensor 1 and sensor 3					
Sensor	2	24.0376	12.019	375.44	2.20E-16
Residuals	20	0.6403	0.032		
Road Sect. 1: EB2 sensor 2 and sensor 4					
Sensor	2	21.0387	10.5194	406.86	2.20E-16
Residuals	20	0.5171	0.0259		
Road Sect. 2: NB1 sensor 1 and sensor 3					
Sensor	2	33.348	16.6742	615.59	2.20E-16
Residuals	20	0.542	0.0271		
Road Sect. 2: NB1 sensor 2 and sensor 4					
Sensor	2	28.2977	14.1489	553.9	2.20E-16
Residuals	20	0.5109	0.0255		
Road Sect. 2: NB2 sensor 1 and sensor 3					
Sensor	2	33.484	16.7421	604.01	2.20E-16
Residuals	20	0.554	0.0277		
Road Sect. 2: NB2 sensor 2 and sensor 4					
Sensor	2	28.6454	14.3227	479.69	2.20E-16
Residuals	20	0.5972	0.0299		
Road Sect. 1: EB1 sensor 1 and sensor 2					
Sensor	2	22.8455	11.423	326.02	5.45E-16
Residuals	20	0.7007	0.035		
Road Sect. 1: EB1 sensor 3 and sensor 4					
Sensor	2	19.099	9.5495	346.27	3.04E-16
Residuals	20	0.5516	0.0276		
Road Sect. 1: EB2 sensor 1 and sensor 2					
Sensor	2	24.8332	12.4166	478.95	2.20E-16
Residuals	20	0.5185	0.0259		
Road Sect. 1: EB2 sensor 3 and sensor 4					
Sensor	2	20.2431	10.1216	316.86	7.18E-16
Residuals	20	0.6389	0.0319		
Road Sect. 2: NB1 sensor 1 and sensor 2					
Sensor	2	34.721	17.3605	640.94	2.20E-16
Residuals	20	0.542	0.0271		
Road Sect. 2: NB1 sensor 3 and sensor 4					
Sensor	2	26.925	13.4625	527.01	2.20E-16
Residuals	20	0.5109	0.0255		
Road Sect. 2: NB2 sensor 1 and sensor 2					
Sensor	2	34.58	17.2899	591.68	2.20E-16
Residuals	20	0.584	0.0292		
Road Sect. 2: NB2 sensor 3 and sensor 4					
Sensor	2	27.5498	13.7749	485.8	2.20E-16
Residuals	20	0.5671	0.0284		

Sensors 1 and 3, sensors 2 and 4 were placed the same side of the vehicle. Sensors 1 and 2 were placed on the front wheels of the vehicle, sensors 3 and 4 were placed on rear wheels of vehicle

Table 5 Results of ANOVA tests ANCOVA tests for two road sections

Analysis of Variance Table of Sensor and Pavement Temperature Road Sect. 1 (EB1)						
Model	Residual Df	RSS	Df	Sum of Square	F	*P*-value
Simple	50	1.959				
Main effect	49	1.734	1	0.225	6.929	0.012
Interaction effect	45	1.462	4	0.272	2.09	0.097
Analysis of Variance Table of Sensor and Pavement Temperature Road Sect. 1 (EB2)						
Model	Residual Df	RSS	Df	Sum of Square	F	*P*-value
Simple	50	2.094				
Main effect	49	2.014	1	0.08	2.141	0.15
Interaction effect	45	1.691	4	0.322	2.145	0.091
Analysis of Variance Table of Sensor and Pavement Temperature Road Sect. 2 (NB1)						
Model	Residual Df	RSS	Df	Sum of Square	F	*P*-value
Simple	50	2.337				
Main effect	49	2.312	1	0.025	0.617	0.436
Interaction effect	45	1.85	4	0.462	2.808	0.037
Analysis of Variance Table of Sensor and Pavement Temperature Road Sect. 2 (NB2)						
Model	Residual Df	RSS	Df	Sum of Square	F	*P*-value
Simple	50	2.492				
Main effect	49	2.45	1	0.043	0.995	0.324
Interaction effect	45	1.927	4	0.523	3.055	0.026
Analysis of Variance Table of Sensor and Mean Speed Road Sect. 1 (EB1)						
Model	Residual Df	RSS	Df	Sum of Square	F	*P*-value
Simple	20	0.61				
Main effect	19	0.602	1	0.008	0.2954	0.595
Interaction effect	15	0.381	4	0.272	2.176	0.121
Analysis of Variance Table of Sensor and Mean Speed Road Sect. 1 (EB2)						
Model	Residual Df	RSS	Df	Sum of Square	F	*P*-value
Simple	20	0.67				
Main effect	19	0.624	1	0.047	1.872	0.191
Interaction effect	15	0.374	4	0.249	2.498	0.087
Analysis of Variance Table of Sensor and Mean Speed Road Sect. 2 (NB1)						
Model	Residual Df	RSS	Df	Sum of Square	F	*P*-value
Simple	20	0.85				
Main effect	19	0.776	1	0.074	2.106	0.167
Interaction effect	15	0.53	4	0.245	1.733	0.195
Analysis of Variance Table of Sensor and Mean Speed Road Sect. 2 (NB2)						
Model	Residual Df	RSS	Df	Sum of Square	F	*P*-value
Simple	20	0.805				
Main effect	19	0.726	1	0.079	2.409	0.142
Interaction effect	15	0.495	4	0.231	1.749	0.192

Df represents degrees of freedom and RSS represents residual sum of squares

Table 6 Coefficients of interaction terms from ANCOVA test of two road sections

Summary of Coefficients Road Sect. 1 (EB1)				
	Estimate	Standard Error	t value	*p*-value
Sensor1: Pavement temperature	0.006	0.003	2.097	0.042
Sensor2: Pavement temperature	0.007	0.003	2.359	0.023
Sensor3: Pavement temperature	0.006	0.003	2.110	0.040
Sensor4: Pavement temperature	0.002	0.003	0.816	0.419
Summary of Coefficients Road Sect. 1 (EB2)				
	Estimate	Standard Error	t value	*p*-value
Sensor1: Pavement temperature	0.006	0.003	1.890	0.065
Sensor2: Pavement temperature	0.008	0.003	2.438	0.019
Sensor3: Pavement temperature	0.008	0.003	2.289	0.027
Sensor4: Pavement temperature	0.003	0.003	0.879	0.384
Summary of Coefficients Road Sect. 2 (NB1)				
	Estimate	Standard Error	t value	*p*-value
Sensor1: Pavement Temperature	0.007	0.003	2.281	0.027
Sensor2: Pavement Temperature	0.009	0.003	2.708	0.010
Sensor3: Pavement Temperature	0.010	0.003	3.005	0.004
Sensor4: Pavement Temperature	0.006	0.003	1.818	0.076
Summary of Coefficients Road Sect. 2 (NB2)				
	Estimate	Standard Error	t value	*p*-value
Sensor1: Pavement Temperature	0.008	0.003	2.437	0.019
Sensor2: Pavement Temperature	0.009	0.003	2.882	0.006
Sensor3: Pavement Temperature	0.010	0.003	3.076	0.004
Sensor4: Pavement Temperature	0.006	0.003	1.929	0.060

Table 7 Results of ANOVA tests ANCOVA tests based on winter data

Analysis of Variance Table Road Sect. 1 (EB1)						
Model	Residual Df	RSS	Df	Sum of Square	F	*P*-value
Simple	20	0.610				
Main effect	19	0.602	1	0.008	0.2954	0.595
Interaction effect	15	0.381	4	0.272	2.176	0.121
Analysis of Variance Table Road Sect. 1 (EB2)						
Model	Residual Df	RSS	Df	Sum of Square	F	*P*-value
Simple	20	0.670				
Main effect	19	0.624	1	0.047	1.872	0.191
Interaction effect	15	0.374	4	0.249	2.498	0.087
Analysis of Variance Table Road Sect. 2 (NB1)						
Model	Residual Df	RSS	Df	Sum of Square	F	*P*-value
Simple	20	0.850				
Main effect	19	0.776	1	0.074	2.106	0.167
Interaction effect	15	0.530	4	0.245	1.733	0.195
Analysis of Variance Table Road Sect. 2 (NB2)						
Model	Residual Df	RSS	Df	Sum of Square	F	*P*-value
Simple	20	0.805				
Main effect	19	0.726	1	0.079	2.409	0.142
Interaction effect	15	0.495	4	0.231	1.749	0.192

Df represents degrees of freedom and RSS represents residual sum of squares

Table 8 Summary of threshold values

Month	EB1 M1	EB1 M2	EB1 M3	EB1 M4	EB2 M1	EB2 M2	EB2 M3	EB2 M4	Mean
3	2.04	1.35	2.2	1.63	1.62	1.61	1.89	1.66	1.75
4	2.62	1.64	1.72	1.73	1.6	1.38	1.27	1.65	1.7
5	2.55	2.32	2.35	1.77	2.15	1.94	1.96	1.45	2.06
6	3.31	2.71	2.15	2.2	2.8	2.54	1.8	2.23	2.47
8	2.66	2.33	3.71	1.74	2.34	2.5	3.41	1.76	2.56
9	1.12	1.77	2.43	1.87	0.99	2.09	2.11	1.85	1.78
10	2.05	1.7	2.1	1.64	1.62	1.85	1.97	1.67	**1.83**
11	1.87	1.65	2.17	1.89	1.57	1.67	2.06	1.8	**1.84**
12	1.9	1.3	2.15	1.92	1.6	1.42	1.92	2.02	**1.78**
1	1.6	1.83	1.79	1.4	2.25	1.52	1.7	1.82	**1.74**
2	1.57	1.48	2.17	1.89	1.55	1.51	2.19	1.77	**1.77**
Month	NB1 M1	NB1 M2	NB1 M3	NB1 M4	NB2 M1	NB2 M2	NB2 M3	NB2 M4	Mean
3	1.42	1.13	1.74	1.37	1.32	1.07	1.6	1.32	1.37
4	1.26	0.94	1.03	1.18	1.22	0.91	0.95	0.92	1.05
5	1.5	1.25	1.47	1.11	1.53	1.34	1.58	1.24	1.38
6	2.16	1.45	1.32	1.49	2.01	1.35	1.24	1.36	1.55
8	1.27	2.11	2.04	1.63	1.3	2.32	2.05	1.62	1.79
9	1.05	1.52	1.69	1.55	0.91	1.48	1.58	1.51	1.41
10	1	1.41	1.45	1.3	1.03	1.3	1.44	1.25	**1.27**
11	1.23	1.28	1.66	1.3	1.22	1.19	1.55	1.24	**1.33**
12	1.25	1.14	1.52	1.47	1.2	1.14	1.5	1.46	**1.34**
1	1.09	1.22	1.35	1.04	1.18	1.22	1.17	1.14	**1.18**
2	1.07	1.06	1.72	1.37	1	1.09	1.71	1.42	**1.31**

M1 to M4 represent sensors 1 to 4. The first row represents the month in the pavement sensing work

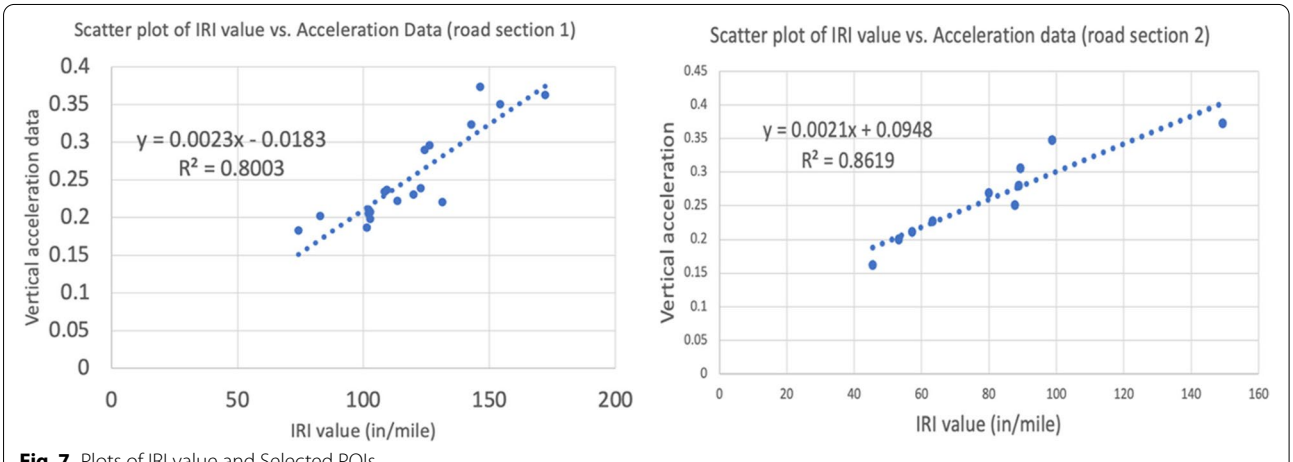

Fig. 7 Plots of IRI value and Selected POIs

Acknowledgements
The authors acknowledge Mr. Manuel Lopez jr. and Jimmie Devany, former undergraduate students at Northern Arizona University, for their work in IRI and POI correlation.

Authors' contributions
Dada Zhang: Conceptualization, Data curation, Formal analysis, Investigation, Methodology, Software, Roles/Writing—original draft. Chun-Hsing Ho: Funding acquisition, Project administration, Resources, Supervision, Visualization, Writing—review & editing. Fangfang Zhang: Data curation, Investigation, Validation, Software, Roles/Writing—original draft. The author(s) read and approved the final manuscript.

Funding
The authors would like to express their gratitude for the grant support by the Pacific Southwest Region 9 University Transportation Center's Craig Roberts Fellowship.

Availability of data and materials
Some or all data, models, or code generated or used during the study are proprietary or confidential in nature and may only be provided with restrictions including, vibration datasets, Excel files, Statistical software codes, GIS mapping data, etc. Data requests will be reviewed based on the corresponding author's discretion.

Declarations

Competing interests
The authors declare that they have no competing interests.

Author details
[1]Durham School of Architectural Engineering and Construction, College of Engineering, University of Nebraska – Lincoln, Lincoln, NE 68588, USA. [2]Department of Mathematical Science, Michigan Technological University, Houghton, MI 49931, USA.

Received: 11 October 2022 Revised: 6 November 2022 Accepted: 8 November 2022
Published online: 03 January 2023

References

1. McGhee KK (2000) Quality assurance of road roughness measurement final report. Virginia Transportation Research Council. Available via RPSA P. https://rosap.ntl.bts.gov/view/dot/19515 document. Accessed 2021.
2. Douangphachanh V, Oneyama H (2013) Using smartphones to estimate road pavement condition. In: International Symposium for Next Generation Infrastructure, Wollongong, Australia, 1–4 Oct 2013.
3. Gogoi R, Dutta B (2020) Maintenance prioritization of interlocking concrete block pavement using fuzzy logic. Int J Pavement Res Technol 13(2):168–175
4. Janani L, Sunitha V, Mathew S (2021) Influence of surface distresses on smartphone-based pavement roughness evaluation. Int J Pavement Eng 22(13):1637–1650
5. Prażnowski K, Mamala J, Śmieja M, Kupina M (2020) Assessment of the road surface condition with longitudinal acceleration signal of the car body. Sensors 20(21):5987
6. Vemuri V, Ren Y, Gao L, Lu P, Song L (2020) Pavement condition index estimation using smartphone based accelerometers for city of Houston. In: Construction Research Congress 2020: Infrastructure Systems and Sustainability, Reston, VA: American Society of Civil Engineers, 9 Nov 2019, pp 522–531.
7. Ho CH, Snyder M, Zhang D (2020) Application of vehicle-based sensing technology in monitoring vibration response of pavement conditions. J Transp Eng 146(3):04020053. https://doi.org/10.1061/JPEODX.0000205
8. Zhang D, Ho CH, Zhang F (2021) Using regression analysis and distribution fitting to analyze pavement sensing patterns for condition assessments. Paper presented at 2021 Transportation Research Board Annual Meeting, Washington, DC, January. TRBAM-21–04008.
9. Gkyrtis K, Loizos A, Plati C (2021) Integrating pavement sensing data for pavement condition evaluation. Sensors 21(9):3104
10. Zoccali P, Loprencipe G, Galoni A (2017) Sampietrini stone pavements: distress analysis using pavement condition index method. Appl Sci 7(7):669
11. Yan G, Wang L, Ye Z, Wang W (2020) Effects of crack damage on acceleration response of asphalt pavement via numerical analysis. J Mater Civ Eng 32(7):04020163
12. Alavi AH, Buttlar WG (2018) Smartphone technology integrated with machine learning for airport pavement condition assessment. Data Analytics for Smart Cities. Auerbach Publications, pp 1–22.
13. Du R, Qiu G, Gao K, Hu L, Liu L (2020) Abnormal road surface recognition based on smartphone acceleration sensor. Sensors 20(2):451
14. Kim HJ, Han JY, Lee S, Kwag JR, Kuk MG, Han IH, Kim MH (2020) A road condition classification algorithm for a tire acceleration sensor using an artificial neural network. Electronics 9(3):404
15. Mandal V, Mussah AR, Adu-Gyamfi Y (2020) Deep learning frameworks for pavement distress classification: A comparative analysis. In: 2020 IEEE International Conference on Big Data (Big Data), 10–13 Dec, pp 5577–5583.
16. Özdemir OB, Soydan H, Yardımcı Çetin Y, Düzgün HŞ (2020) Neural network based pavement condition assessment with hyperspectral images. Remote Sensing 12(23):3931
17. Rana S, Asaduzzaman MB, Saha B, Azam M (2019) Vibration based pavement condition monitoring using smartphone as a sensor. In: International Conference on Planning, Architecture and Civil Engineering (ICPACE), Rajshahi University of Engineering & Technology, Rajshahi, Bangladesh, 7–9 Feb 2019.
18. Staniek M (2021) Road pavement condition diagnostics using smartphone-based data crowdsourcing in smart cities. J Transp Eng 8(4):554–567
19. Zhong M, Sui L, Wang Z, Hu D (2020) Pavement crack detection from mobile laser scanning point clouds using a time grid. Sensors 20(15):4198
20. Mohideen AJH, Rosli MF, Hanif NHHM, Zaki HFM, Husman MA, Muthalif AGA, Kumar D (2020) Pavement condition analysis via vehicle mounted accelerometer data. IIUM Eng J 21(1):73–84
21. Gong H, Sun Y, Shu X, Huang B (2018) Use of random forests regression for predicting IRI of asphalt pavements. Constr Build Mater 189:890–897
22. Singh AP, Sharma A, Mishra R, Wagle M, Sarkar AK (2018) Pavement condition assessment using soft computing techniques. Int J Pavement Res Technol 11(6):564–581
23. Chuang TY, Perng NH, Han JY (2019) Pavement performance monitoring and anomaly recognition based on crowdsourcing spatiotemporal data. Autom Constr 106:102882
24. Staniek M (2018) Repeatability of road pavement condition assessment based on three-dimensional analysis of linear accelerations of vehicles. In: IOP Conference Series: Materials Science and Engineering, vol 356, IOP Publishing, p 012021.
25. Kyriakou C, Christodoulou SE, Dimitriou L (2019) Do vehicles sense pavement surface anomalies. In: European Conference on Computing in Construction (EC3), Chania, Crete, Greece, 10 Jul 2019.
26. Kuehl RO (2000) Design of experiments: statistical principles of research design and analysis. Duxbury press.
27. Bates D. Compute Tukey honest significant differences. R Documentation. Available via R Documentation. https://stat.ethz.ch/R-manual/R-patched/library/stats/html/TukeyHSD.html document. Accessed 2021.
28. Faraway JJ (2004) Linear models with R. Chapman and Hall/CRC
29. Grogg M (2017) Overview of performance measures: pavement condition to assess the national highway performance program. Transportation Performance Management. https://www.fhwa.dot.gov/policyinformation/presentations/hisconf/thu01_hpms_and_tpm-part_1_overview_of_performance_measures-pavement_condition_max_grogg.pdf document. Accessed 2022.

Publisher's Note